PUBLICATIONS OF THE ASTRONOMICAL SOCIETY OF THE PACIFIC, **125**:644–653, 2013 June

Ionization within the Local Cavity by Hot White Dwarfs

BARRY Y. WELSH,[1] JONATHAN WHEATLEY,[1] NATHAN J. DICKINSON,[2] AND MARTIN A. BARSTOW[2]

Received 2013 April 17; accepted 2013 May 01; published 2013 May 28

ABSTRACT. We present estimates of the contribution from 33 nearby ($d < 100$ pc) hot DA white dwarfs to the total ionization of the Local Cavity. The EUV spectra of these white dwarfs have been derived using non-LTE stellar atmosphere models (with the inclusion of metals where necessary) to calculate the incident flux at the Earth using up-to-date distances and interstellar column densities. Our model spectra give a very good approximation to the spectra obtained with observations from the NASA *Extreme Ultraviolet Explorer* satellite. The number of Lyman continuum photons per second emitted by each of the white dwarfs for wavelengths over the 30–912 Å range was then derived. Using these numbers, the respective sizes of the ionized Strömgren spheres of HII were then calculated for each star under the assumption of ambient interstellar electron density values of $n_e = 0.04$ cm^{-3} and 0.10 cm^{-3}. The location and sizes of these ionized regions have been plotted on a 3D map of the neutral absorption contours of the local ISM, as derived for both in-plane and out of plane directions. A similar procedure was also carried out for the determination of the sizes of the ionized HeII regions surrounding the same 33 white dwarfs. We conclude that only a few of the very hottest DA white dwarfs located within the Local Cavity can possess appreciably sized ionized Strömgren spheres of HII and HeII. The size of these ionized regions can potentially range between 20 pc and 40 pc in diameter, dependent on the ambient value of the electron density of the interstellar medium. However, the volumetric filling factor of these ionized spheres within the Local Cavity is small (~6%), even at the lowest value of electron density considered in this study (i.e., $n_e = 0.04$ cm^{-3}). Thus, the contribution from DA white dwarfs to the ionization of both the local interstellar cloud complex and other clouds located within the Local Cavity is of secondary importance compared to the ionization contribution provided by the two early B-type stars of ϵ and β CMa.

1. INTRODUCTION

The Sun resides in a very low neutral interstellar density region of the Galaxy called the Local Cavity (also known as the Local Bubble), whose physical properties have been summarized by Frisch & Redfield (2011). The dimensions of this low density region have been mapped using both HI (Vergely et al. 2001), dust (Vergely et al. 2010) and NaI and CaII absorption (Welsh et al. 2010a), such that it is now known to have a highly asymmetric shape ranging from 30 to 150 pc from the Sun before encountering a dense and cold neutral gas boundary in most Galactic directions. There are many low density (n(HI) ~ 0.1 cm^{-3}), partially ionized (n_e ~ 0.1 cm^{-3}) and warm (T ~ 7000 K) cloudlets located within 30 pc of the Sun, the most well-studied being the local interstellar cloud complex ($d < 5$ pc), within which the Sun is thought to partially reside (Lallement et al. 1986; Lallement & Bertin 1992; Redfield & Linsky 2008). Although having being studied at many wavelengths for over 40 years, there is still debate as to the nature of the rarefied gas that presumably exists between these embedded cloudlets and thus fills the remaining volume of the large interstellar cavity (Welsh & Shelton 2009).

Observations of the soft X-ray $1/4$ keV background emission have long been interpreted as originating in a local million degree gas thought to fill the Local Cavity (McCammon & Sanders 1990; Snowden et al. 1998). However, with the recognition that emission from solar wind charge-exchange can dominate this background signal, very low limits have now been placed on the contribution to the $1/4$ keV background from a hot local gas residing at mid-plane latitudes (Koutroumpa et al. 2009, 2011; Peek et al. 2011). In contrast, at high Galactic latitudes where the Local Cavity opens up into the lower halo, the observed soft X-ray emission presumably originates in a ubiquitous hot and highly ionized halo gas (Welsh & Shelton 2009). Ultraviolet (UV) absorption measurements towards several B-type stars and hot white dwarfs located within 100 pc have revealed absorption from the high ions of SiIV, CIV and OVI that has been associated with an interstellar origin (Huang et al. 1995; Savage & Lehner 2006; Welsh & Lallement 2008, 2010). While SiIV and CIV are thought to form through photoionization of the local interstellar gas at temperatures ~10^5 K, the OVI ion traces higher temperature gas at ~3×10^5 K, which is thought to be collisionally excited in the turbulent transition zones between the (purported) million kelvin soft X-ray emitting local plasma and the cooler gas

[1]Experimental Astrophysics Group, Space Sciences Laboratory, University of California, Berkeley, CA 94720.

[2] Department of Physics and Astronomy, University of Leicester, Leicester LE1 7RH, UK.

cloudlets residing therein. In addition, the ubiquitous detection of absorption by MgII, FeII, CII and SiII ions throughout the Local Cavity has generally been interpreted as supporting the widespread presence of photoionized gas with a temperature of $\sim 10^4$ K (Redfield & Linsky 2002, 2004).

The possibility of high ions originating in the ionization spheres surrounding local hot white dwarfs was first realized by Dupree & Raymond (1983). Their calculations showed that large volumes of ionized gas containing substantial column densities of highly ionized species could exist over long recombination times in the interstellar environment around hot, hydrogen-rich white dwarfs. Later work on the interpretation of highly ionized absorption features occurring at nonphotospheric velocities in the UV spectra of local hot white dwarfs by Bannister et al. (2003) favored mass loss as an origin rather than interstellar. However, a recent reanalysis of high ion absorption detected towards local hot white dwarfs suggests that many of the high ion absorption lines previously identified with an interstellar origin may in fact be of a circumstellar origin (Lallement et al. 2011; Dickinson et al. 2012a). This notion is supported in part by the observed temporal variability of these absorption lines, which in some cases has been attributed to the evaporation of orbiting dusty solid bodies (such as asteroids) that aperiodically fall towards the central star. In addition, there is an observed anticorrelation between the white dwarf stellar temperature and the high ion velocity shift with respect to the photosphere. Such a dependence would therefore favor a circumstellar, rather than an interstellar, origin for a significant fraction of these high ion absorptions (Lallement et al. 2011). Alternately, some of these high ions could be associated with an origin within the ionized Strömgren spheres that surround DA white dwarfs, and hence could be termed nebular, as opposed to interstellar lines (Dickinson et al. 2012b).

Since there are many hot ($T > 20,000$ K) white dwarfs located within the known confines of the Local Cavity (i.e., within $\sim$100 pc of the Sun), we can determine if they could have any appreciable effect on the ionization of the purported filler gas within the Local Cavity. Previous attempts to determine the ionization sources of the Local Cavity have concentrated on the observed ionization state of the local cloud complex (Vallerga 1998; Slavin & Frisch 2002, 2008; Slavin 2011). Observations by the *Extreme Ultraviolet Explorer* (*EUVE*) satellite revealed that the local ionizing field measured at the Earth is completely dominated by two early B stars (ϵ and β CMa) for $500\ \text{Å} < \lambda < 912\ \text{Å}$ and by three hot white dwarfs for $200\ \text{Å} < \lambda < 500\ \text{Å}$ (Vallerga 1998). Photoionization calculations that include radiation from these nearby hot stars, the extreme ultraviolet (EUV) emission from the (purported) million kelvin gas responsible for the diffuse soft X-ray background and from a possible evaporative boundary between the 7000 K local clouds and the million kelvin gas, have successfully matched the ionization and heating requirements of the local gas (Slavin & Frisch 2002, 2008). However, such calculations were based on observational constraints that required a significant contribution from the assumed presence of a million kelvin, soft X-ray emitting, diffuse local gas. At distances beyond the local cloud complex, very little is known concerning the ionization of more distant cloudlets located within the Local Cavity (Redfield & Falcon 2008; Welsh & Lallement 2010), although there is some evidence that the level of hydrogen ionization increases along the general direction of the rarefied interstellar tunnel towards Canis Major (Wolff et al. 1999).

In the maps of the distribution of partially ionized interstellar gas within 300 pc, it was noted that the Local Cavity appeared to contain a honeycomb of small cell-like subcavities bounded by thin gas filaments that might be associated with ionized stellar HII regions formed by the stellar wind action of B-type and/or hot white dwarfs (Welsh et al. 2010a). Although it was uncertain whether these features were a byproduct of the three-dimensional (3D) mapping software program, it was conjectured that such ionized cavities could be a potential source of the highly ionized nebular absorption lines observed within the local interstellar medium (ISM). This has prompted us to reevaluate the possible role of hot white dwarfs in forming ionization spheres dispersed throughout the Local Cavity, as first suggested by Dupree & Raymond (1983). An estimate of the sole contribution from hot white dwarfs within 20 pc to the ionization of the local interstellar medium (LISM) by ultraviolet radiation was presented by Tat & Terzian (1999) based on the sizes of white dwarf Strömgren spheres. This analysis showed that the total ionization was irregular and did not consist of one large ionized cloud, but instead was the result of irregular regions of ionization with occasional mergers between the white dwarf ionized spheres. Since publication of the Tat & Terzian (1999) paper, many of the white dwarf distances and stellar temperatures have been updated; the dimensions of the Local Cavity are now well known, and the ambient interstellar gas densities now have improved estimates. Hence, in this article we reevaluate the ambient contribution of hot white dwarfs to the total ionization of the Local Cavity and present the 3D spatial distribution of their ionized Strömgren spheres in Galactic coordinate plots. It should be emphasized that these are only localized effects within the Local Cavity, since the dominant sources of photoionization of the local ISM as measured *at the Earth* are the two early B-type stars of ϵ and β CMa, of which the former emits nine times more EUV flux longward of 600 Å. Calculations also show that ϵ CMa alone produces a hydrogen photoionization rate at the Earth of $1.1 \times 10^{-15}\ \text{s}^{-1}$, which is a factor of 6 higher than the *total* from all nearby stars (Cassinelli et al. 1995). In fact, given the extremely low neutral column density of hydrogen ($N(\text{HI}) < 10^{18}\ \text{cm}^{-2}$) along the line-of-sight towards ϵ CMa, it is highly likely that the local cloud complex may be considered as actually residing within its ionized Strömgren sphere.

2. HOT WHITE DWARF ISM IONIZATION

2.1. Strömgren Spheres

The work of Tat & Terzian (1999) only considered the effects of the ionization from the Strömgren spheres of the known white dwarfs with (pre-*Hipparcos*) distances less than 20 pc. The great majority of these sources possessed stellar temperatures $<20,000$ K, with correspondingly small ionization spheres of radii less than a few parsecs. Based on the recent absorption maps of the Local Cavity (Welsh & Lallement 2010), it is clear that there are many hot ($T > 20,000$ K) white dwarfs with distances up to at least 100 pc that presumably have significantly larger Strömgren spheres that, in principle, may be providing a nonnegligible contribution to the total ionization of the Local Cavity. In Table 1, we list 33 white dwarfs with temperatures $>20,000$ K and with distances $<100 \pm 5$ pc, as presented by Barstow et al. (2010). It should be noted that this list is not inclusive of all the DA white dwarfs that meet our temperature and distance criteria, but it represents the majority of those that have been well-studied at ultraviolet wavelengths and whose stellar properties are well-known. The table gives the white dwarf name, Galactic position, (post-*Hipparcos*) distance, stellar effective temperature ($T_{\rm eff}$) and the stellar gravity $\log g$. The stellar radii ($R_{\odot}$) values were adopted from the work of Wood (1995), and for a white dwarf not included in that paper, we list a radius value for a star of similar $\log g$ and $T_{\rm eff}$. In Figure 1, we plot the positions of these sources with respect to the neutral boundary of the Local Cavity in the mid-plane projection, as determined from NaI absorption observations (Welsh & Lallement 2010). In order to view all 33 sources in Table 1, we have projected the positions of each of the targets onto the Galactic plane at the position of their Galactic longitude, irrespective of their Galactic latitude. It is clear from the projection of Figure 1 that the vast majority of the 33 targets lie within the rarefied confines of the Local Cavity.

The radius of a Strömgren sphere depends on two important sets of parameters: the stellar temperature and radius, and the electron temperature and density of the ambient interstellar gas (Strömgren 1939; Panagia 1973). It is now well established that metals are present in the atmospheres of hot DA white

TABLE 1

STELLAR PROPERTIES, IN ORDER OF INCREASING $T_{\rm eff}$

Star	l (deg)	b (deg)	Distance (pc)	$T_{\rm eff}$ (K)	$\log g$	Radius ($R_{\odot}$)
WD 0512+326	173.30	−3.36	25.0	22,750.0	8.01	0.01366
WD 2014−575	340.20	−34.25	51.0	26,579.0	7.78	0.01623
WD 2020−425	358.36	−34.45	52.0	28,597.0	8.54	0.00903
WD 1041+580	150.12	52.17	93.0	29,016.0	7.79	0.01620
WD 0830−535	270.11	−8.27	82.0	29,330.0	7.79	0.01621
WD 0147+674	128.58	5.44	99.0	30,120.0	7.70	0.01734
WD 1844−223	12.50	−9.25	62.0	31,470.0	8.17	0.01225
WD 0235−125	165.97	−50.27	86.0	32,306.0	8.44	0.00985
WD 0549+158	192.03	−5.34	49.0	32,780.0	7.83	0.01585
WD 0236+498	140.15	−9.15	96.0	33,822.0	8.47	0.00961
WD 0050−332	299.14	−84.12	58.0	34,684.0	7.89	0.01521
WD 1109−225	274.78	34.54	82.0	36,750.0	7.50	0.02058
WD 2257−073	65.17	−56.93	89.0	38,010.0	7.84	0.01590
WD 1254+223	317.25	84.75	67.0	38,205.0	7.90	0.01519
WD 1615−154	358.79	24.18	55.0	38,205.0	7.90	0.01519
WD 1611−084	4.30	29.30	93.0	38,500.0	7.85	0.01579
WD 2111+498	91.37	1.13	50.0	38,866.0	7.84	0.01592
WD 1302+597	119.82	57.59	79.0	39,960.0	8.31	0.01103
WD 0346−011	188.95	−40.10	29.0	42,373.0	9.00	0.00576
WD 1440+753	114.10	40.12	98.0	42,400.0	8.54	0.00909
WD 2004−605	336.58	−32.86	58.0	44,200.0	8.14	0.01271
WD 0715−704	281.40	−23.50	94.0	44,300.0	7.69	0.01808
WD 1631+781	111.30	33.58	67.0	44,559.0	7.79	0.01673
WD 0001+433	113.90	−18.44	99.0	46,205.0	8.85	0.00681
WD 0004+330	112.48	−28.69	99.0	47,936.0	7.77	0.01710
WD 1314+293	54.11	84.16	68.0	49,435.0	7.95	0.01487
WD 2309+105	87.26	−45.12	79.0	51,300.0	7.91	0.01539
WD 2331−475	334.84	−64.81	82.0	56,682.0	7.64	0.01934
WD 0501+524	155.95	7.10	59.0	57,340.0	7.48	0.02221
WD 0621−376	245.41	−21.43	78.0	62,280.0	7.22	0.02839
WD 0232+035	165.97	−50.27	74.0	62,947.0	7.53	0.02157
WD 2211−495	345.79	−52.62	53.0	65,600.0	7.42	0.02395
WD 2350−706	309.91	−45.94	92.0	69,300.0	8.00	0.01463

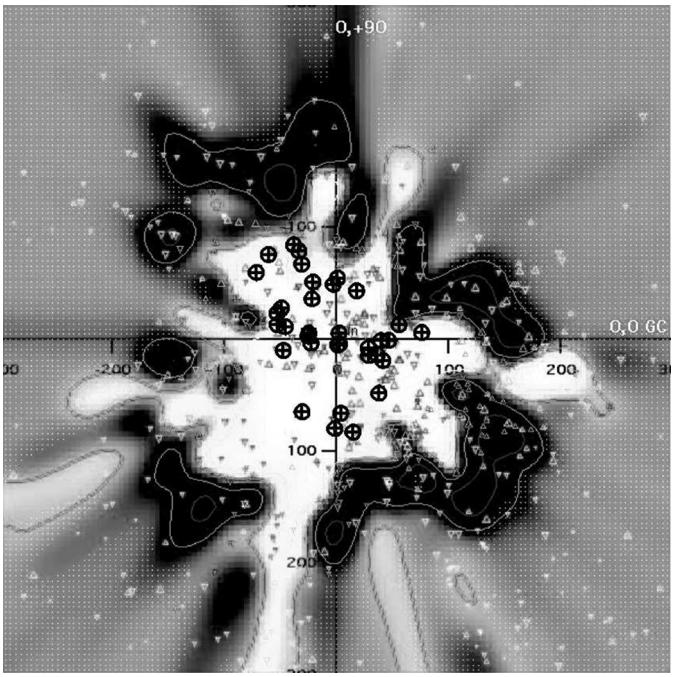

FIG. 1.—Plot of the galactic distribution of the 33 local hot white dwarfs (⊕) considered in this article. The stars are superposed on an absorption map of the Local Cavity within 300 pc of the Sun at mid-plane latitudes (Welsh & Lallement 2010). *White* to *dark* shading represents low to high values of neutral interstellar gas density. The Galactic latitudes of all stars have been projected onto the mid-plane for ease of viewing. Note that all of the targets lie within the rarefied Local Cavity. *Small triangles* represent the stars whose interstellar NaI observations were used to create the absorption map.

dwarfs due to radiative levitation (Chayer et al. 1995), such that stars with $T_{\rm eff}$ values higher than $\sim 50,000$ K contain significant quantities of Fe peak elements (Barstow et al. 2003). Appreciable UV line blanketing is caused by these peak elements which, together with the absorption at discrete UV wavelengths by lower mass ions, has a nonnegligible effect on their Strömgren sphere sizes (Dickinson et al. 2012a). In order to fully account for these effects, it is necessary to model each DA white dwarf stellar atmosphere, taking into account the effect of photospheric metals. This represents a significant improvement over the previous works of Dupree & Raymond (1983) and Tat & Terzian (1999).

2.2. Stellar Model Atmospheres

Models for each white dwarf were constructed using the values of $T_{\rm eff}$ and $\log g$ listed in Table 1, using the non-LTE stellar atmosphere code TLUSTY (Hubeny & Lanz 1995). Helium was included in the model atmospheres of the coolest ($T_{\rm eff} < 55,000$ K) white dwarfs with a homogenous depth distribution and an abundance of $\rm He/H = 10^{-5}$, since this broadly reproduces the observations of most DA white dwarfs (Barstow et al. 2003). For the case of HZ 43, a well-known, pure-H hot white dwarf, He was included with $\rm He/H = 3.2 \times 10^{-7}$, following the analysis of *EUVE* data (Barstow et al. 1997). To reproduce the observed low wavelength (<240 Å) EUV flux distribution of the hottest white dwarfs (i.e., $T_{\rm eff} > 55,000$ K), He was included following the method described by Barstow & Hubeny (1998), with the EUV spectra of the white dwarfs well reproduced with a hydrogen layer mass of $\log(\delta M/M) = -12.99$.

All metals were homogeneously distributed in the model atmospheres, where present. Where photospheric C, N, O, Si and Ni have been identified (Barstow et al. 2003), they were included at the abundance stated therein. However, the N abundance for WD $0050-332$ and WD $1611-084$ were taken from Dickinson et al. (2012a), and the C and S abundances for WD $0050-332$, G191-B2B (WD $0501+524$) and WD $1611-084$ were taken from Dickinson et al. (2013), as these studies provide more up-to-date abundance values. The elements of P and S were included in the models at the levels found by Barstow et al. (2013, in preparation). The inclusion of Fe at the abundances derived from far-ultraviolet (FUV) absorption line profile analyses (such as Barstow et al. 2003) predicted excessive flux for wavelengths <200 Å; using a higher abundance of $\rm Fe/H = 3 \times 10^{-5}$ in conjunction with a stratified He configuration prevented such a short wavelength excess. Exceptions were WD $2111+498$ and WD $2309+105$, where the lower Fe abundances taken from Vennes et al. (2006) and Vennes & Dupuis (2002) better matched the observations (since the radiative levitation of Fe is weaker in stars with $T_{\rm eff} < 55,000$ K). Si, P and S abundances were included in the model of WD $2350-706$ at the abundances found by Barstow et al. (2013, in preparation). Since no C, N, O, Fe or Ni abundances have been published for this star, we assumed the abundances of G191-B2B for those elements, taking that star to be a representative hot DA.

Finally, in addition to the aforementioned stellar atmosphere parameters, the incident flux at the Earth also depends on the interstellar gas column densities of neutral hydrogen, *N*(H) and neutral helium, *N*(HeI), in addition to ionized helium, *N*(HeII). For all cases, we have used the model of Rumph et al. (1994) to account for the absorption by both interstellar H and He along the path length to each star (see Table 1 for the distances assumed for each white dwarf). The *EUVE* observations of HZ 43 (WD $1314+293$) are well reproduced by our model in Figure 2 under the assumption of $N_{\rm HI} = 0.83 \times 10^{18}$ cm^{-2}, $N_{\rm HeI} = 0.65 \times 10^{17}$ cm^{-2} and $N_{\rm HeII} = 0.41 \times 10^{17}$ cm^{-2} (Barstow et al. 1997). In Figure 3, we similarly show the *EUVE* observations of G191-B2B (WD $0501+524$) and our stellar model assuming $N_{\rm HI} = 2.05 \times 10^{18}$ cm^{-2}, $N_{\rm HeI} = 2\times 10^{17}$ cm^{-2} and $N_{\rm HeII} = 5.97 \times 10^{17}$ cm^{-2} (Barstow et al. 1999, 2005). In Figure 4, for the case of Feige 24 (WD $0232+035$), we similarly show the *EUVE* observations being well matched by our model that assumes $N_{\rm HI} = 2.79 \times 10^{18}$ cm^{-2}, $N_{\rm HeI} = 1.56 \times 10^{17}$ cm^{-2} and $N_{\rm HeII} = 3.9 \times 10^{17}$ cm^{-2} (Barstow et al. 1999; Kowalski et al. 2011). We note that there are slight deviations between observations and model at short wavelengths for HZ 43 and between 300 Å and 450 Å for Feige 24.

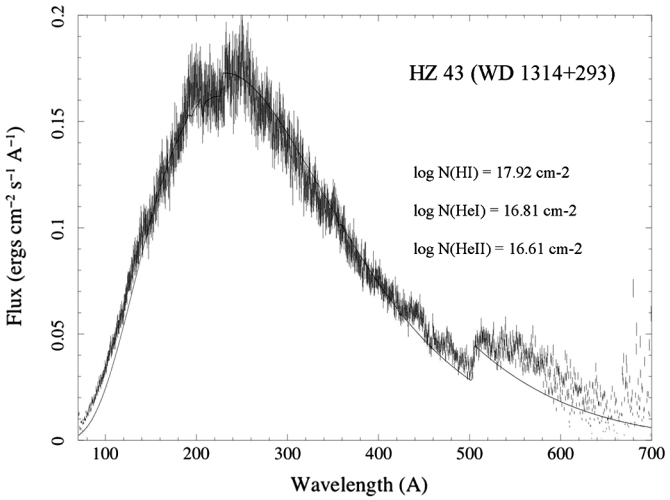

FIG. 2.—Observed spectrum of HZ 43 recorded by the *EUVE* satellite (*heavy line*) superposed with a model atmosphere (*solid light line*) as described in § 2.

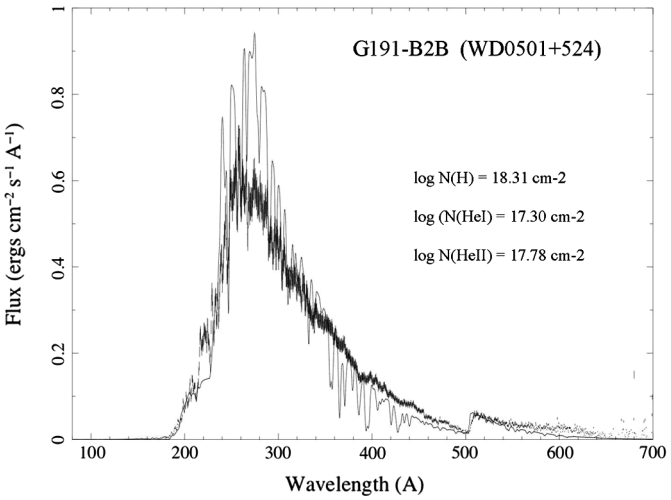

FIG. 3.—Observed spectrum of G191-B2B recorded by the *EUVE* satellite (*heavy line*) superposed with a model atmosphere (*solid light line*) as described in § 2.

Differences in the values of $T_{\rm eff}$ and $\log g$ assumed in this study, compared with previous studies from which He and metal abundances and interstellar column density values were derived, probably explain the minor deviations seen in the spectra of HZ 43 and Feige 24. Our current understanding of the Fe atomic transitions that give rise to significant opacity at EUV wavelengths (Preval et al. 2013) and uncertainty of the true depth distribution of Fe (Barstow et al. 1999) may also contribute. A detailed investigation of these effects are beyond the scope of this present work, and will be explored in a later study. However, it is clear from the fits to the *EUVE* spectra of the three hot white dwarfs shown in Figures 2–4 that our current models give a good approximation to the observed spectra and, as such, we can proceed with confidence to derive the number of Lyman continuum photons emitted by each of the 33 stars.

2.3. Emitted Lyman Continuum Photons

The 33 newly calculated white dwarf model atmosphere spectra were then synthesized over the wavelength range of 30–912 Å using the SYNSPEC code (Lanz & Hubeny 2012) in order to calculate the total number of Lyman continuum photons emitted from each star. The SYNSPEC output spectra have fluxes expressed as $F_\lambda(\mathrm{erg\,cm^{-2}\,s^{-1}\,\AA^{-1}\,sr^{-1}})$, which were then converted to a flux (f_λ) of photons $\mathrm{cm^{-2}\,s^{-1}\,\AA^{-1}}$ using the standard conversion of

$$f_\lambda(\mathrm{photons\,cm^{-2}\,s^{-1}\AA^{-1}}) = 5.03\times10^{7}\lambda F_\lambda 4\pi,$$

which, when the surface area of stellar radius, R, is accounted for, gives the total number of Lyman photons emitted per second from 30 Å to 912 Å of

$$\mathrm{photons\ s^{-1}} = \int 5.03\times10^{7}\lambda F_\lambda 4\pi R^2 \delta\lambda.$$

In Table 2, we list the total number of emitted photons $\mathrm{s^{-1}}$ for wavelengths $<$912 Å (the HI Lyman edge) and also for wavelengths $<$504 Å (the HeI edge) for each of the 33 white dwarfs. These numbers will be used subsequently in the determination of the size of each white dwarf Strömgren sphere in § 4. The summed ionizing flux $<$504 Å from the hottest ($T > 45,000$ K) white dwarfs in Table 2 is $\sim$1.6$\times$ 10^{45} photons $\mathrm{s^{-1}}$. For comparison purposes, the Lyman continuum flux emitted $<$912 Å by a typical B2I star (i.e., ϵ CMa) is $\sim10^{46.2}$ photon $\mathrm{s^{-1}}$ (Panagia 1973), which is a factor of 30 greater flux than any of the hot white dwarfs listed in Table 2.

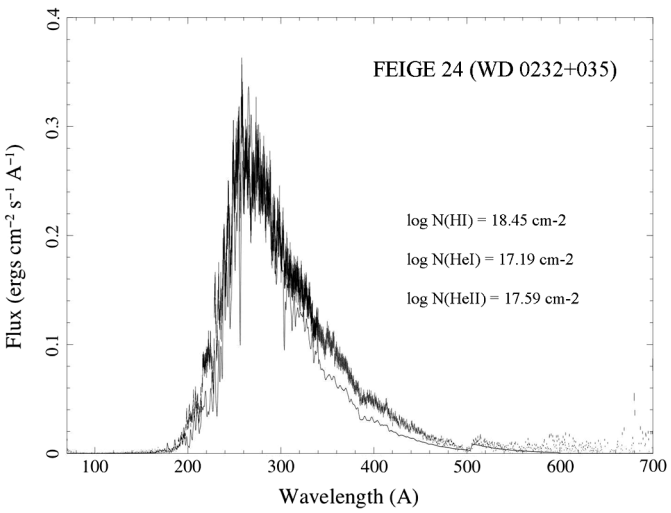

FIG. 4.—Observed spectrum of Feige 24 recorded by the *EUVE* satellite (*heavy line*) superposed with a model atmosphere (*solid light line*) as described in § 2.

TABLE 2

STELLAR FLUXES AND STRÖMGREN HII REGION RADII AT INTERSTELLAR ELECTRON DENSITIES OF $n_e = 0.10$ cm^{-3} AND 0.04 cm^{-3}; STARS LISTED IN ORDER OF INCREASING TEMPERATURE

Star	$T_{\rm eff}$ (K)	$\log_{10}$ Flux ≤ 912 Å (photon s^{-1})	$\log_{10}$ Flux ≤ 504 Å (photon s^{-1})	HII Radius (pc) $n_e = 0.1$ cm^{-3}	HII Radius (pc) $n_e = 0.04$ cm^{-3}
WD 0512+326	22,750	39.51	38.56	0.22	0.41
WD 2014−575	26,579	40.69	40.08	0.54	1.00
WD 2020−425	28,597	40.85	40.41	0.62	1.13
WD 1041+580	29,016	41.38	40.88	0.92	1.70
WD 0830−535	29,330	41.47	40.97	0.99	1.83
WD 0147+674	30,120	41.75	41.25	1.22	2.25
WD 1844−223	31,470	41.84	41.38	1.31	2.41
WD 0235−125	32,306	41.85	41.42	1.33	2.44
WD 0549+158	32,780	42.32	41.86	1.89	3.49
WD 0236+498	33,822	42.10	41.68	1.61	2.96
WD 0050−332	34,684	42.74	42.32	2.63	4.85
WD 1109−225	36,750	43.13	42.71	3.53	6.51
WD 2257−073	38,010	43.05	42.65	3.32	6.11
WD 1254+223	38,205	43.03	42.63	3.27	6.02
WD 1615−154	38,205	43.03	42.63	3.27	6.02
WD 1611−084	38,500	43.09	42.70	3.43	6.32
WD 2111+498	38,866	43.13	42.75	3.54	6.53
WD 1302+597	39,960	42.91	42.54	2.99	5.50
WD 0346−011	42,373	42.53	42.20	2.23	4.11
WD 1440+753	42,400	42.92	42.58	3.02	5.56
WD 2004−605	44,200	43.32	42.99	4.10	7.56
WD 0715−704	44,300	43.63	43.30	5.20	9.59
WD 1631+781	44,559	43.58	43.25	5.00	9.21
WD 0001+433	46,205	42.90	42.59	2.96	5.45
WD 0004+330	47,936	43.78	43.48	5.82	10.73
WD 1314+293	49,435	43.72	43.44	5.58	10.27
WD 2309+105	51,300	43.84	43.56	6.10	11.23
WD 2331−475	56,682	44.31	44.03	8.71	16.05
WD 0501+524	57,340	44.44	44.13	9.69	17.86
WD 0621−376	62,280	44.87	44.59	13.47	24.81
WD 0232+035	62,947	44.65	44.37	11.32	20.85
WD 2211−495	65,600	44.81	44.56	12.86	23.69
WD 2350−706	69,300	44.49	44.26	10.07	18.55

3. CONTRIBUTIONS TO THE STELLAR EUV RADIATION FIELD

The integrated stellar radiation field at the Earth, as measured at extreme ultraviolet wavelengths (85–912 Å), is shown in Figure 5, and this spectrum represents the summed contributions from the observed EUV spectra of 54 stars (Vallerga 1998). Superposed on this figure we show the major contributors at wavelengths >500 Å that arise from two early B stars (ϵ and β CMa), both of which are located along an interstellar tunnel of very low neutral gas density (Welsh 1991). For wavelengths in the 200–450 Å range, three hot white dwarfs (HZ 43, G191-B2B and Feige 24) are the major contributors. As noted in § 2, the majority of hot white dwarfs (apart from the singular case of HZ 43) provide almost no ionizing flux for wavelengths <200 Å. Thus, it seems likely that an assortment of nearby stellar sources (such as cataclysmic variables and active late-type stars) may account for the observed short wavelength flux of the EUV radiation field.

Clearly the EUV field measured at other locations within the Local Cavity will differ from that shown in Figure 5. However, although the level of observed flux will be different at other Galactic locations, it seems likely that the major stellar contributors will still be very similar, such that the two early Bstars will remain the dominant contributors of ionizing flux for wavelengths >500 Å throughout the Local Cavity.

4. STRÖMGREN SPHERE SIZES

Although we acknowledge the importance of both ϵ and β CMa with regard to the total ionization of the local interstellar hydrogen gas for wavelengths >500 Å, our present study is aimed at the more localized effects of hot white dwarfs. In order to determine the actual size of the ionized HII region surrounding each white dwarf, in addition to knowledge of their stellar ionizing flux (as derived in § 2), we also require information on the physical state of the ambient interstellar medium. In particular, the ambient neutral interstellar density determines the

potential size of an idealized Strömgren sphere. This value determines the radius at which HII ionized gas, defined by the gas electron density, n_e, becomes neutralized. Integrated values for n_e have been measured along many sightlines within the Local Cavity (Redfield & Falcon 2008; Welsh & Lallement 2010), but actual ambient values (apart from that of the local cloud complex) are essentially unknown. However, based on the maximum and minimum values reported by Lehner et al. (2003) for a sample of 30 hot white dwarfs within 200 pc, we make the assumption that, within the Local Cavity, $0.04\ \mathrm{cm}^{-3} < n_e < 0.10\ \mathrm{cm}^{-3}$ is typical for most of the ambient interstellar plasma. Such a range of electron density values are not unreasonable for many other sightlines measured within the local ISM (Redfield & Falcon 2008), but are a factor of 4 greater than the values of n_e used by Tat & Terzian (1999). Had we used a value of $n_e = 0.01\ \mathrm{cm}^{-3}$ for the interstellar gas surrounding some of the very hottest of the local white dwarfs, this would have resulted in Strömgren sphere sizes that would have completely filled the Local Cavity, which we deem is probably an unreasonable assumption.

In Table 2 we list the radii of the (idealized) Strömgren spheres for ionized hydrogen, together with the stellar fluxes (in photons s^{-1}) for wavelengths <912 Å and also for wavelengths <504 Å (the HeI edge). We note that for hot white dwarfs with temperatures $\gtrsim 45,000$ K, the number of photons emitted <504 Å per star is approximately equal to half of the total number of photons emitted <912 Å by that star. When summed together, the total ionizing flux <504 Å from these hottest white dwarfs is $\sim 1.6 \times 10^{45}$ photons s^{-1}. The ramifications of the flux from the hottest white dwarfs to the ionization of interstellar helium gas are discussed in § 5.1.

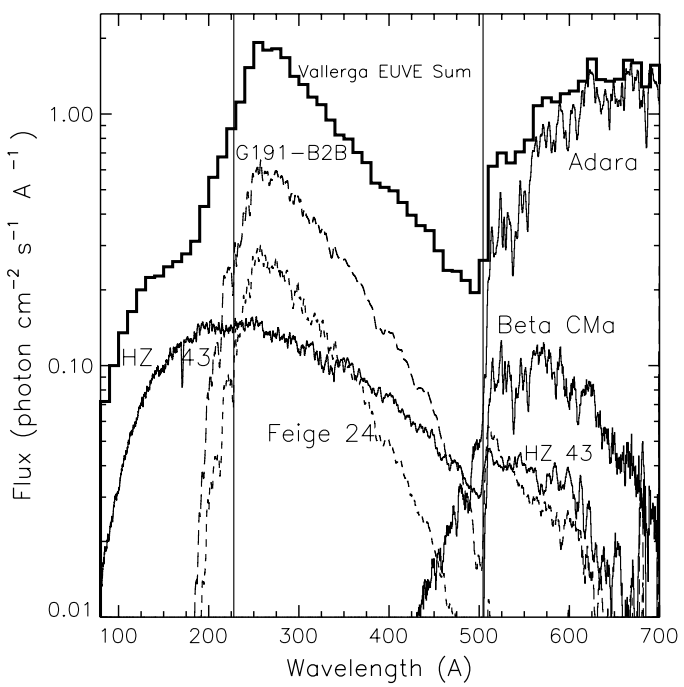

FIG. 5.—Stellar EUV radiation field (80–912 Å) at the Earth, as measured by the *Extreme Ultraviolet Explorer* satellite (Vallerga 1998). For wavelengths >500 Å, it is dominated by contributions from two early type-B stars (ϵ and β CMa), and for wavelengths >500 Å, local hot white dwarfs are the major contributor.

5. WHITE DWARF IONIZATION WITHIN THE LOCAL CAVITY

Inspection of Table 2 shows that locally ionized bubbles of hydrogen with diameters greater than 10 pc should not be totally uncommon within the Local Cavity, even at the highest values of ambient gas density considered here. Assuming that there is no overlap between these ionized spheres, their total volume amounts to 2.6×10^5 pc^3 for an assumed value of electron density, $n_e = 0.04\ \mathrm{cm}^{-3}$, and a volume of 4.2×10^4 pc^3 for $n_e = 0.10\ \mathrm{cm}^{-3}$. The total volume of the Local Cavity (assuming it approximates a sphere of 100 pc radius) is $\sim 4.2 \times 10^6$ pc^3. Thus, even for the lowest assumed value of ambient electron density the (maximum) volumetric filling factor of these ionized regions is only 6%.

In Figure 6 we show the location and sizes of the HII regions surrounding the 14 hot white dwarfs located within $\pm 30°$ of the Galactic plane superposed on the map of mid-plane neutral gas absorption observed within 300 pc (Welsh & Lallement 2010). It is clear from this plot that at mid-plane latitudes there are no nearby hot white dwarfs that would have any measurable effect on the ionization of the local clouds, even under the assumption of the lowest value of ambient electron density considered here. Only one source, WD $0621-376$, has any appreciably sized HII region in the mid-plane and, serendipitously, the sightline to this star is similar to that of the two (more distant) early B-type stars (β and ϵ CMa) that are located within the rarefied extension to the Local Cavity. Since these two stars are known to dominate the EUV ionizing flux (>500 Å) at the Earth, any contribution from the HII region of WD $0621-376$ will thus be masked by the two B stars' far larger combined ionizing flux.

In Figure 7 we show the location and sizes of the HII regions of the 19 hot white dwarfs at Galactic latitudes away from the mid-plane (i.e., $+30° < b < -30°$). We see again that there are no hot white dwarfs within close proximity to the local cloud complex that might significantly affect its ionization state. However, at distances >50 pc in the general direction of ($l \sim 330°$, $b \sim -50°$), a cluster of three white dwarfs (WD $2211-495$, WD $2331-475$ and WD $2350-706$) may well have a measurable effect on the ionization of the ambient medium. However, this apparent local excess of ionization is not reflected in maps of Hα emission (Finkbeiner 2003) or in the OVI absorption measurements of Barstow et al. (2010) towards these stars. This could be due to a higher value of ambient electron density than that used in our present calculations, which would reduce the sizes of the ionized regions surrounding these stars.

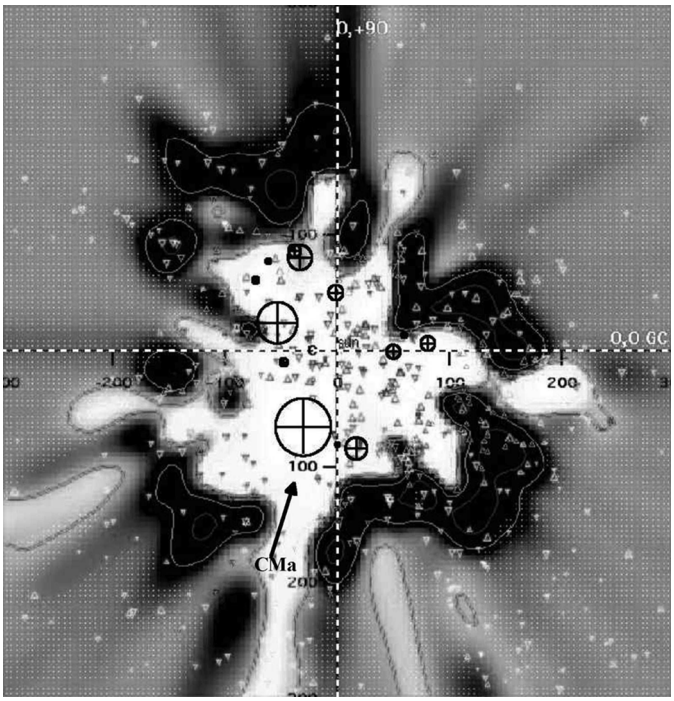

FIG. 6.—Location and sizes of the Strömgren spheres of ionized hydrogen surrounding 14 hot DA white dwarfs located at mid-plane latitudes (±30°) within the Local Cavity, under the assumption of an ambient electron density, $n_e = 0.04$ cm^{-3}. The spheres have been superposed on an absorption map of the Local Cavity at mid-plane latitudes within 300 pc of the Sun (Welsh & Lallement 2010). The position of rarefied CMa interstellar tunnel, which contains the two early B stars ϵ and β CMa that are the main contributors to the ionization of the local ISM, is also indicated.

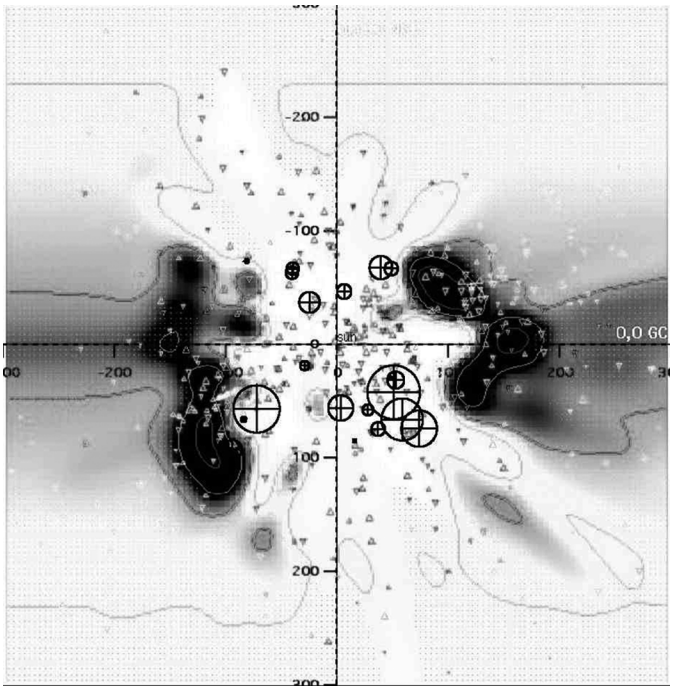

FIG. 7.—Location and sizes of the Strömgren spheres of ionized hydrogen surrounding 19 hot DA white dwarfs located at latitudes $+30° < b < -30°$ above the mid-plane within the Local Cavity, under the assumption of an ambient electron density, $n_e = 0.04$ cm^{-3}. The spheres have been superposed on an absorption map of the Local Cavity, as viewed in the meridian plane within 300 pc of the Sun (Welsh & Lallement 2010).

5.1. Ionization of Helium

The interstellar abundance of Ar I, as measured towards several nearby hot white dwarfs, has been found to be significantly below its cosmic abundance relative to H I (Jenkins et al. 2000). This is thought to be due to some Ar being present in the ionized state of ArII, which requires photons with an ionization potential of >15.8 eV. It is expected that Ar should be more strongly ionized than H because the cross section for the photoionization of Ar I is very high. Similarly, a surprisingly high ionization of He (compared with that of H) has also been measured within the LISM (Dupuis et al. 1995; Barstow et al. 1997). Along sightlines where interstellar absorption from HeII λ228 is detected, the ionization fractions are not correlated with viewing direction nor with the sightline column density (Barstow et al. 1997). The fairly constant values of He and H ionization fractions found throughout the local ISM are consistent with the predictions of Lyu & Bruhweiler (1996), based on time-dependent ionization calculations of the local gas following shock heating from a nearby supernova event.

Unfortunately, none of the known stellar sources that contribute to the observed EUV ionization field can adequately explain this excess of He ionization (Vallerga 1998). It has been proposed that the EUV/soft X-ray emission radiated from an evaporative interface at the boundary of the local cloud could provide a natural extra source of the hard ionizing photons needed to explain the observed high level of He ionization (Slavin & Frisch 2002). However, this model assumes that CIVλ1548 should be detectable at levels of $N(\mathrm{CIV}) \sim 1 \times 10^{12}$ cm^{-2} in many sightlines through the local clouds, in contrast with observations that have failed to detect widespread CIV absorption within the local ISM (Welsh & Shelton 2009; Welsh et al. 2010b). Instead, a radiation burst from a nearby supernova, which elevated the local ionization level but has yet to recombine, has recently been forwarded as a potential alternative source of flux with an ionization potential >24.6 eV that can elevate HeI to HeII (Jenkins 2013).

A complete analysis of the size of an ionized HeII Strömgren sphere surrounding a hot white dwarf would require step-by-step radiation transfer calculations that take account of the passage of HeII photons through the inner ionized HII region. This is beyond the current scope of this article, but for simplicity let us now assume that for white dwarfs with temperatures $>45,000$ K, the HeII ionized regions are of similar size to their respective HII Strömgren spheres (Osterbrock & Ferland 2006). Table 2 suggests that the hottest white dwarfs can provide

$\sim 1.6 \times 10^{45}$ photon s^{-1} at wavelengths <504 Å. Thus, in the absence of H, there would appear to be sufficient high energy photons to ionize HeI to HeII. However, since there are 10 times more H atoms than He atoms in the local interstellar gas, most of these high energy photons from the hottest white dwarfs are absorbed by H and not He. If we now visually replace the HII region sizes shown in Figures 6 and 7 with comparably sized HeII ionized regions, we again see that the volumetric contribution of ionization from these regions is small ($\sim 6\%$), and none of them are sufficiently near to the local cloud complex to serve as a potential source for the observed overionization of HeII.

6. CONCLUSIONS

Although it is well established that the major contributors to the ionization of the local interstellar cloud complex are the two B-type stars ϵ and β CMa, we have investigated whether local hot DA white dwarfs can provide a significant contribution to ionization at other Galactic locations within the Local Cavity. Therefore, we have estimated the contribution from 33 nearby ($d < 100$ pc) hot DA white dwarfs to the total ionization of the Local Cavity. This has been achieved by modeling each of the white dwarf's EUV spectral output with a non-LTE stellar atmosphere with the inclusion of metals where necessary. The incident flux at the Earth was then derived for each of the 33 stars using up-to-date distances and interstellar column densities. Our model spectra give a very good approximation to the spectra obtained with the NASA *Extreme Ultraviolet Explorer* satellite. The number of Lyman continuum photons per second emitted by each of the white dwarfs for wavelengths over the 30–912 Å was then derived. Using these numbers, the respective sizes of the ionized Strömgren spheres of HII were then calculated for each star under the assumption of interstellar electron density values of $n_e = 0.04$ cm^{-3} and 0.10 cm^{-3}. The location and sizes of these ionized regions were then plotted on a 3D map of the neutral absorption contours of the local ISM, as derived for both in-plane and out of plane directions. A similar procedure was also carried out for the determination of the sizes of the ionized HeII regions surrounding the 33 white dwarfs. For all cases, it was found that the volumetric contribution to the total ionization of the local ISM from the DA white dwarfs was small ($\sim 6\%$) compared to the far larger contribution from the two early type-B stars ϵ and β CMa.

In the general Galactic direction of ($l \sim 330°$, $b \sim -50°$), our calculations indicate that there could be an apparent local excess of ionization due to the close proximity of ionized regions surrounding the three white dwarfs WD $2211-495$, WD $2331-475$ and WD $2350-706$. However, such a predicted excess is not reflected in Hα emission or interstellar OVI absorption observations.

Thus, we conclude that only the (few) very hottest DA white dwarfs located within the Local Cavity can possess appreciably sized ionized Strömgren spheres of HII and HeII. The size of these ionized regions can potentially range between 20 pc and 40 pc in diameter, dependent on the ambient value of electron density. However, the volumetric filling factor of these ionized spheres is small even at the lowest value of electron density considered in this study (i.e., $n_e = 0.04$ cm^{-3}). Thus, the contribution from DA white dwarfs to the hydrogen ionization of both the local interstellar cloud complex and other clouds located within the Local Cavity is negligible compared to the ionizing flux provided by the two early B-type stars of ϵ and β CMa.

BYW would like to acknowledge *HST*-COS Guaranteed Time Observer funding for this research through NASA GSFC grant 005118. NJD and MAB acknowledge the support of the UK Science and Technology Facilities Council. Amazingly useful conversations and suggestions were gained from John Vallerga, Jeff Linsky and Rosine Lallement.

REFERENCES

Bannister, N., Barstow, M., Holberg, J., & Bruhweiler, F. 2003, MNRAS, 341, 477
Barstow, M., Boyce, D., Welsh, B. Y., Lallement, R., Barstow, J. K., Forbes, A. E., & Preval, S. 2010, ApJ, 723, 1762
Barstow, M., Cruddace, R., Kowalski, M., et al. 2005, MNRAS, 362, 1273
Barstow, M., Dobbie, P., Holberg, J., Hubeny, I., & Lanz, T. 1997, MNRAS, 286, 58
Barstow, M., Good, S., Holberg, J., Hubeny, I., Bannister, N. P., Bruhweiler, F. C., Burleigh, M. R., & Napiwotzki, R. 2003, MNRAS, 341, 870
Barstow, M., & Hubeny, I. 1998, MNRAS, 299, 379
Barstow, M., Hubeny, I., & Holberg, J. 1999, MNRAS, 307, 884
Cassinelli, J., Cohen, D., MacFarlane, J., et al. 1995, ApJ, 438, 932
Chayer, P., Fonatine, G., & Wesemael, F. 1995, ApJS, 99, 189
Dickinson, N., Barstow, M., Welsh, B. Y., Burleigh, M., Farihi, J., Redfield, S., & Unglaub, K. 2012a, MNRAS, 423, 1397
Dickinson, N., Barstow, M., & Hubeny, I. 2012b, MNRAS, 421, 3222
Dickinson, N., Barstow, M., & Welsh, B. Y. 2013, MNRAS, 428, 1873
Dupree, A., & Raymond, J. 1983, ApJ, 275, L71
Dupuis, J., Vennes, S., Bowyer, S., Pradhan, A. K., & Thejll, P. 1995, ApJ, 455, 574
Finkbeiner, D. P. 2003, ApJS, 146, 407
Frisch, P., & Redfield, S. 2011, ARA&A, 49, 237
Huang, J-S., Songaila, A., & Cowie, L. 1995, ApJ, 450, 163
Hubeny, I., & Lanz, T. 1995, ApJ, 439, 875
Koutroumpa, D., Lallement, R., Raymond, J., & Kharchenko, V. 2009, ApJ, 696, 1517
Koutroumpa, D., Smith, R. K., Edgar, R., Kuntz, K. D., Plucinsky, P. P., & Snowden, S. L. 2011, ApJ, 726, 91
Kowalski, M., Barstow, M., Wood, K., et al. 2011, ApJ, 730, 115
Jenkins, E. 2013, ApJ, 764, 25
Jenkins, E., Oegerle, W., Gry, C., et al. 2000, ApJ, 538, L81

Lallement, R., & Bertin, P. 1992, A&A, 266, 479
Lallement, R., Vidal-Madjar, A., & Ferlet, R. 1986, A&A, 168, 225
Lallement, R., Welsh, B. Y., Barstow, M., & Casewell, S. 2011, A&A, 533, 140
Lanz, T., & Hubeny, I. 2012, SYNSPEC Version 43, http://nova.astro.umd.edu/Synspec43/synspec.html
Lehner, N., Jenkins, E., Gry, C., Moos, H. W., Chayer, P., & Lacour, S. 2003, ApJ, 595, 858
Lyu, C-H., & Bruhweiler, F. 1996, ApJ, 459, 216
McCammon, D., & Sanders, W. 1990, ARA&A, 28, 657
Osterbrock, D. E., & Ferland, G. J. 2006, Astrophysics of Gaseous Nebulae and Active Galactic Nuclei (Mill Valley: Univ. Science Books)
Panagia, N. 1973, AJ, 78, 929
Peek, J., Heiles, C., Peek, K., Meyer, D. M., & Lauroesch, J. T. 2011, ApJ, 735, 129
Preval, S., Barstow, M., Holberg, J., & Dickinson, N. 2013, in ASP Conf. Ser. 469, 18th European White Dwarf Workshop, ed. J. Krzesinski, G. Stachowski, P. Moskalik, & K. Bajan (San Francisco: ASP), 193
Redfield, S., & Falcon, R. 2008, ApJ, 683, 207
Redfield, S., & Linsky, J. 2002, ApJS, 139, 439
Redfield, S., & Linsky, J. 2004, ApJ, 602, 776
Redfield, S., & Linsky, J. 2008, ApJ, 673, 283
Rumph, T., Bowyer, S., & Vennes, S. 1994, AJ, 107, 2108
Savage, B., & Lehner, N. 2006, ApJS, 162, 134
Slavin, J. 2011, in AIP Conf. Proc. 1366, Partially Ionized Plasmas throughout the Cosmos—Proceedings of the 2010 Huntsville Worshop, ed. V. Florinski, J. Heerikhuisen, G. P. Zank, & D. L. Gallagher (New York: AIP), 89
Slavin, J., & Frisch, P. 2002, ApJ, 565, 364
Slavin, J., & Frisch, P. 2008, A&A, 491, 53
Snowden, S., Egger, R., Finkbeiner, D., Freyberg, M. J., & Plucinsky, P. P. 1998, ApJ, 493, 715
Strömgren, B. 1939, ApJ, 89, 526
Tat, H., & Terzian, Y. 1999, PASP, 111, 1258
Vallerga, J. V. 1998, ApJ, 497, 921
Vennes, S., & Dupuis, J. 2002, in ASP Conf. Ser. 262, The High Energy Universe at Sharp Focus: Chandra Science, ed. E. M. Schlegel, & S. D. Vrtilek (San Francisco: ASP), 57
Vennes, S., Chayer, P., Dupuis, J., & Lanz, T. 2006, ApJ, 652, 1554
Vergely, J-L., Freire Ferrero, R., Siebert, A., & Valette, B. 2001, A&A, 366, 1016
Vergely, J-L., Valette, B., Lallement, R., & Raimond, S. 2010, A&A, 518, 31
Welsh, B. Y. 1991, ApJ, 373, 556
Welsh, B. Y., & Lallement, R. 2008, A&A, 490, 707
Welsh, B. Y., & Lallement, R. 2010, PASP, 122, 1320
Welsh, B. Y., Lallement, R., Vergely, J-L., & Raimond, S. 2010a, A&A, 510, 54
Welsh, B. Y., Wheately, J., Siegmund, O. H. W., & Lallement, R. 2010b, ApJ, 712, L199
Welsh, B. Y., & Shelton, R. 2009, Ap&SS, 323, 1
Wolff, B., Koester, D., & Lallement, R. 1999, A&A, 346, 969
Wood, M. A. 1995, in Proc. 9th European Workshop on White Dwarfs, White Dwarfs, ed. D. Koester, & K. Werner (Heidelberg: Springer-Verlag Berlin), 41